Inorg. Chem. **2007**, *46*, 9450–9462

Synthesis, Structure, Spectral and Electrochemical Properties, and Catalytic Use of Cobalt(III)–Oxo Cubane Clusters

Rajesh Chakrabarty, Sanchay J. Bora, and Birinchi K. Das*

Department of Chemistry, Gauhati University, Guwahati 781 014, Assam, India

Received June 16, 2007

Olive-green cobalt(III) complexes having the general formula $Co_4O_4(O_2CMe)_4L_4$ (**1**) where L = py (**1a**), 4-Mepy (**1b**), 4-Etpy (**1c**), and 4-CNpy (**1d**) have been prepared by the H_2O_2 oxidation of a mixture of Co^{2+}, $MeCO_2^-$, and pyridine or 4-substituted pyridines in a 1:2:1 molar ratio in methanol. Spectroscopic and X-ray crystallographic studies show that these complexes contain a tetrameric cubane-like core $[Co_4(\mu_3\text{-}O)_4]^{4+}$ where the four cobalt atoms form an approximate tetrahedron with edge lengths of ~2.75 Å. Each cobalt in the crystallographically determined structure of $Co_4(\mu_3\text{-}O)_4(\mu\text{-}O_2CMe)_4L_4$ in **1a**·$NaClO_4$·3.5H_2O and **1b**·3H_2O is hexacoordinate. Infrared spectra of the complexes show characteristic bands near 700, 635, and 580 cm^{-1} due to the central cubane-like core. ^1H NMR spectra of the complexes show that the dissolved species are essentially diamagnetic and also that the complexes maintain their integrity in solution. UV–vis spectra of the green solutions have been interpreted in terms of ligand-field and charge-transfer bands. The electrochemical behavior of the complexes studied by cyclic and differential pulse voltammetric techniques indicates that the $[(Co^{III})_4(\mu_3\text{-}O)_4]^{4+}$ core present in the complexes undergoes a reversible one-electron oxidation to the $[(Co^{III})_3Co^{IV}(\mu_3\text{-}O)_4]^{5+}$ core with an $E_{1/2}$ value below 1 V. This suggests that these complexes of cobalt may be suitable as catalysts for the oxidation of organic compounds. Preliminary investigations indicate that **1a** has a role to play in the cobalt-catalyzed aerobic oxidation of neat ethylbenzene and *p*-xylene.

Introduction

Oxo-bridged transition-metal carboxylate clusters with ancillary N- and O-donor ligands are of continuing interest for the synthetic inorganic chemists, partly because of their complex and varied structural motifs, and also due to their magnetic, optical, and catalytic properties as well as biological relevance.[1] The most common core units encountered in such tetranuclear clusters are $[M_4(\mu_3\text{-}O)_2]$ (**I**), $[M_4(\mu_3\text{-}O)_3]$ (**II**), and $[M_4(\mu_3\text{-}O)_4]$ (**III**).

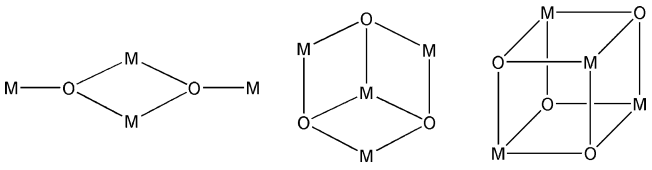

Studies on oxo-carboxylato cobalt clusters having a cubane-like core have stemmed from their interesting structural, spectroscopic, magnetic, and catalytic properties. Christou et al. isolated the first such complex of cobalt(III), viz. $[Co_4O_4(O_2CMe)_2(bpy)_4]^{2+}$ (bpy = 2,2′-bipyridine) by dimerizing the dinuclear complex $[Co_2(\mu\text{-}OH)_2(\mu\text{-}O_2CMe)(\eta^1\text{-}O_2CMe)_2(bpy)_2]^+$ with Li_2O_2 in hot dimethylsulfoxide (DMSO).[2] The complex has a cuboidal $[(Co^{III})_4(\mu_3\text{-}O)_4]^{4+}$ core of type **III** with cobalt and oxygen atoms occupying alternate vertices. The complex $Co_4O_4(O_2CMe)_4(py)_4$ having the same $[Co_4O_4]^{4+}$ core was isolated by Beattie et al. from a mixture of several other species by direct ozonolysis of cobalt(II) acetate in H_2O/AcOH/pyridine followed by precipitation with NH_4PF_6.[3] PbO_2 has been used to oxidize Co^{2+} for the synthesis of a cubane-like tetramer $[Co_4(pg)_4O_4]$ containing *N*-(2-pyridylmethyl)glycinate (pg) as ancillary

* To whom correspondence should be addressed. E-mail: das_bk@rediffmail.com. Phone/Fax: +91 (0)361 2570535.

(1) Winpenny, R. E. P. In *Comprehensive Coordination Chemistry*; McCleverty, J. A.; Meyer, T. J., Eds.; Pergamon Press: Oxford, 2004; Vol. 7, Chapter 7.3, pp. 125−175. Winpenny, R. E. P. *Adv. Inorg. Chem.* **2001**, *52*, 1−111.
(2) Dimitrou, K.; Folting, K.; Streib, W. E.; Christou, G. *J. Am. Chem. Soc.* **1993**, *115*, 6432−6433.
(3) Beattie, J. K.; Hambley, T. W.; Klepetko, J. A.; Masters, A. F.; Turner, P. *Polyhedron* **1998**, *17*, 1343−1354.

10.1021/ic7011759 CCC: $37.00
Published on Web 10/02/2007

ligands.[4] Alkoxo-bridged[5] as well as hydroxo-bridged[6] tetranuclear clusters are also reported in the literature.

From the catalytic point of view, oxo-bridged transition-metal-cluster complexes of cobalt are of particular interest because of their usefulness and relevance toward the autoxidation of various aromatic hydrocarbons. Oxo-centered trinuclear cobalt clusters,[7] $[(py)_3Co_3O(OAc)_5OR][PF_6]$, have been used as catalytic precursors for the autoxidation of toluene in acetic acid containing LiBr with O_2 as the oxidant to produce benzoic acid.[8] Ratnasamy et al. have demonstrated[9] the catalytic oxidation of *p*-xylene to terephthalic acid by trinuclear oxo-bridged cluster complexes of cobalt in the presence of dioxygen. The related complex $[Mn_4O_4(Ph_2PO_2)_6]$ and its analogue $[Mn_4O_4(O_2P(p\text{-}MePh)_2)_6]$ were also shown to catalyze the oxidation of a variety of substrates such as thioethers, hydrocarbons, alkenes, benyzl alcohol, and benzaldehyde with *tert*-butyl hydroperoxide (TBHP) as the oxidant.[10]

Our interests on cobalt(III) cubane-like clusters of the type $Co_4O_4(O_2CR)_4L_4$, where R is a methyl or an aryl group and L is either a pyridine or a substituted pyridine ligand, are due to their role in the catalyzed oxidation of organic substrates such as alkylaromatics, alcohols, and α-pinene, a bicyclic monoterpene with air, oxygen, or TBHP as the oxidants.[11−15] Herein, we describe a general method for the synthesis of cubane-like cobalt(III) tetramers $Co_4O_4(O_2CMe)_4L_4$ with L = pyridine (py, **1a**), 4-methylpyridine (4-Mepy, **1b**), 4-ethylpyridine (4-Etpy, **1c**), or 4-cyanopyridine (4-CNpy, **1d**) and their structural, spectral, and electrochemical properties. The crystal structure of the compound **1a**·$0.5NaNO_3$·$8H_2O$ has been reported[13] by us in connection with the use of a heterogeneous catalyst, prepared by immobilizing **1a** on chemically modified mesoporous silica, for the TBHP oxidation of several primary and secondary alcohols. Presently, we also describe the crystal structure of another modification of **1a** in the form of **1a**·$NaClO_4$·$3.5H_2O$, which presents an interesting supramolecular structure type along with that of a related compound **1b**·$3H_2O$.

The complex $Co_4(\mu_3\text{-}O)_4(\mu\text{-}O_2CMe)_4(4\text{-}CNpy)_4$ (**1d**) was previously described as a catalyst for the oxidation of *p*-xylene in aqueous medium under moderate dioxygen pressure.[12] In that instance, *p*-xylene was found to undergo oxidation to produce mostly *p*-toluic acid along with a trace of terephthalic acid. Presently, we demonstrate that complex **1a** is either a catalyst or a catalyst precursor in the catalyzed oxidation of *p*-xylene and ethylbenzene, both of which are industrially important substrates. Since there is no need to use any additional solvents for the oxidation of these alkylaromatics to form useful organic chemicals, and also because no additives are necessary for carrying out the catalytic reactions under atmospheric pressure, our results also appear to be significant from the green chemistry point of view. The catalytic results are briefly discussed in this paper.

Experimental Section

Materials. All materials used in this work were obtained from commercial sources and used without further purification. $Co(NO_3)_2$·$6H_2O$, sodium acetate trihydrate, and hydrogen peroxide were procured from E. Merck (India). Pyridine (Qualigens, India), 4-methylpyridine and 4-ethylpyridine (E. Merck, Germany), 4-cyanopyridine (Aldrich, U.S.), *p*-xylene (E. Merck, Germany), ethylbenzene (E. Merck, Germany) were all used as received. The methanol used for synthesis was of reagent grade. TBAP was procured from E. Merck, Germany. Dichloromethane used for spectral and electrochemical studies was distilled after drying over P_4O_{10}. Acetonitrile and methanol used for spectral and electrochemical measurements were of HPLC grade.

Measurements. Infrared spectra in the mid-IR region (4000−450 cm^{-1}) were recorded using a Perkin-Elmer RX1 FT-IR spectrophotometer for KBr pellets. UV−vis spectra were recorded on a Perkin-Elmer Lambda 40 spectrophotometer. C, H , N analyses were done using a Perkin-Elmer 2400 Series II CHNS/O analyzer. Cobalt analysis was performed gravimetrically by precipitating out cobalt as $Hg[Co(NCS)_4]$ following standard procedure. Room-temperature magnetic susceptibility was measured using a benchtop Sherwood MK-1 balance. ^1H NMR spectral measurements were made using a Bruker 400 MHz instrument. Tetramethylsilane (TMS) was used as an internal standard. Chemical shifts reported are in parts per million (ppm) taking TMS signal as 0.00 ppm. In order to follow the course of the catalytic oxidation of ethylbenzene, a Hewlett-Packard 6890 series GC equipped with a DB17 capillary column was used.

Electrochemistry. Cyclic and differential pulse voltammetric measurements were performed using (i) an EG&G PAR model 253 VersaStat potentiostat/galvanostat having a three-electrode setup consisting of a glassy-carbon working, platinum-wire auxiliary, and a saturated calomel reference electrode (SCE) combined with electrochemical analysis software 270 for recording the voltammograms; and (ii) a BAS 100B electrochemical analyzer equipped with a BAS C2 cell stand. Electrochemical data were collected and analyzed using *BAS 100W*, version 2.3, software. Cyclic voltammetry (CV) was conducted using a three-electrode cell assembly consisting of a glassy-carbon disc or a platinum disc as the working electrode, a platinum wire as auxiliary electrode, and Ag/AgCl as the reference electrode.

(4) Ama, T.; Okamoto, K.; Yonemura, T.; Kawaguchi, H.; Takeuchi, A.; Yasui, T. *Chem. Lett.* **1997**, 1189−1190.

(5) (a) Bertrand, J. A.; Hightower, T. C. *Inorg. Chem.* **1973**, *12*, 206−210. (b) Wang, R.; Hong, M.; Su, W.; Cao, R. *Acta Crystallogr.* **2001**, *E57*, m325−m327. (c) Olmstead, M. M.; Power, P. P.; Sigel, G. A. *Inorg. Chem.* **1988**, *27*, 580−583. (d) Berchin, E. K.; Harris, S. G.; Parsons, S.; Winpenny, R. E. P. *Chem. Commun.* **1996**, 1439−1440. (e) Gubina, K. E.; Ovchynnikov, V. A.; Swiatek-Kozlowska, J.; Amirkhanov, V. M.; Sliva, T. Y.; Domasevitch, K. V. *Polyhedron* **2002**, *21*, 963−967.

(6) (a) He, C.; Lippard, S. *J. Am. Chem. Soc.* **2000**, *122*, 184−185. (b) Zhao, H.; Bacsa, J.; Dunbar, K. R. *Acta Crystallogr.* **2004**, *E60*, m637−m640.

(7) (a) Sumner, C. E., Jr. *Inorg. Chem.* **1988**, *27*, 1320−1327. (b) Sumner, C. E., Jr.; Steinmetz, G. R. *Inorg. Chem.* **1989**, *28*, 4290−4294.

(8) Sumner, C. E., Jr.; Steinmetz, G. R. *J. Am. Chem. Soc.* **1985**, *107*, 6124−6126.

(9) (a) Chavan, S. A.; Srinivas, D.; Ratnasamy, P. *Chem. Commun.* **2001**, 1124−1125. (b) Chavan, S. A.; Srinivas, D.; Ratnasamy, P. *J. Catal.* **2001**, *204*, 409−419. (c) Chavan, S. A.; Halligudi, S. B.; Srinivas, D.; Ratnasamy, P. *J. Mol. Catal. A: Chem.* **2000**, *161*, 49−64.

(10) Carrell, T. G.; Cohen, S.; Dismukes, G. C. *J. Mol. Catal. A: Chem.* **2002**, *187*, 3−15.

(11) Chakrabarty, R.; Das, B. K.; Clark, J. H. *Green Chem.* **2007**, *9*, 845−848.

(12) Chakrabarty, R.; Kalita, D.; Das, B. K. *Polyhedron* **2007**, *26*, 1239−1244.

(13) Sarmah, P.; Chakrabarty, R.; Phukan, P.; Das, B. K. *J. Mol. Catal. A: Chem.* **2007**, *268*, 36−44.

(14) Chakrabarty, R.; Das, B. K. *J. Mol. Catal. A: Chem.* **2004**, *223*, 39−44.

(15) Das, B. K.; Clark, J. H. *Chem. Commun.* **2000**, 605−606.

All electrochemical studies were carried out at room temperature. The sample solutions were purged with and kept under an atmosphere of N_2. The relevant solvent (CH_2Cl_2 or MeCN) contained a large excess of TBAP as the supporting electrolyte in all measurements. The $E_{1/2}$ values quoted are the midpoints of the forward (anodic, E_{pa}) and reverse (cathodic, E_{pc}) peak potentials [$E_{1/2} = (E_{pc} + E_{pa})/2$]. The reversibility of the redox couples was determined from peak-to-peak separations [$\Delta E_p = E_{pa} - E_{pc}$] observed and by estimating the ratio of the cathodic peak current (i_{pc}) and anodic peak current (i_{pa}) at various scan rates (ν). The stoichiometry of the electron-transfer processes was determined from the peak current measurements using ferrocene as an internal standard.

Preparation of Complexes. $Co_4(\mu_3\text{-}O)_4(\mu\text{-}O_2CMe)_4(py)_4\cdot 0.5NaNO_3\cdot 8H_2O$ (1a·0.5 $NaNO_3$·8H_2O). $Co(NO_3)_2\cdot 6H_2O$ (2.90 g, 10 mmol) and $CH_3CO_2Na\cdot 3H_2O$ (2.7 g, 20 mmol) are stirred in methanol (30 mL) and heated to refluxing temperature, and pyridine (0.08 mL, 10 mmol) is added to the stirred reaction mixture. A portion of 30% hydrogen peroxide (v/v, 5 mL, ~50 mmol) is slowly added to the reaction mixture, and stirring under a refluxing condition is continued for 4 h. The color of the mixture changes from violet to olive green. Dark-green crystals were obtained from the concentrated reaction mixture stored at room temperature for 3 days. Yield: 1.07 g (~40% based on cobalt). IR data (KBr pellet, ν_{max}/cm^{-1}): 3433(s, br), 3117(w), 3081(w), 2930(w), 1654(w), 1637(w), 1608(w), 1533(s), 1486(s), 1450(s), 1402(vs), 1386(vs), 1346(s), 1211(m), 1158(w), 1071(m), 1047 (w), 1019(w), 762(s), 696(s), 634(s), 583(s), and 454(w) (s, strong; m, medium; w, weak, br, broad).

$Co_4(\mu_3\text{-}O)_4(\mu\text{-}O_2CMe)_4(py)_4\cdot NaClO_4\cdot 3.5H_2O$ (1a·$NaClO_4$·3.5H_2O). Dark green prismlike crystals of **1a**·$NaClO_4$·3.5H_2O suitable for X-ray diffraction are obtained by adding a saturated aqueous solution of $NaClO_4$ to the concentrated reaction mixture (obtained as above) and allowing the resultant solution to stand for several days at room temperature. The dried sample was analyzed as **1a**·$NaClO_4$·3.5H_2O. Anal. Calcd for $C_{28}H_{39}N_4O_{19.5}Co_4NaCl$: C, 32.41; H, 3.79; N, 5.40. Found: C, 32.30; H, 3.79; N, 5.21. IR data (KBr pellet, ν_{max}/cm^{-1}) for **1a**·$NaClO_4$·3.5H_2O: 3448(s, br), 3116(w), 3082(w), 2928(w), 1630(m), 1609(m), 1530(vs), 1486(s), 1448(s), 1414(vs), 1346(m), 1212(m), 1147(m), 1093(vs), 763(s), 696(s), 633(s), 583(s), and 453(w).

$Co_4(\mu_3\text{-}O)_4(\mu\text{-}O_2CMe)_4(py)_4\cdot KPF_6\cdot 3H_2O$ (1a·KPF_6·3H_2O). Well-formed crystals of **1a**·KPF_6·3H_2O, having tetragonally compressed octahedral morphology, are obtained in a similar manner by adding a concentrated aqueous solution of KPF_6 in place of $NaClO_4$ to the concentrated reaction mixture. The dried sample was analyzed as **1a**·KPF_6·3H_2O. Anal. Calcd for $C_{28}H_{38}N_4O_{15}Co_4KPF_6$: C, 30.84; H, 3.51; N, 5.14. Found: C, 30.64; H, 3.57; N, 5.24. IR data (KBr pellet, ν_{max}/cm^{-1}) for **1a**·KPF_6·3H_2O: 3406(s, br), 3119(w), 3084(w), 2932(w), 1610(m), 1535(vs), 1487(s), 1450(s), 1411(vs), 1347(m), 1214(m), 1154(m), 1073(m), 1028(vs), 849(vs), 762(s), 696(s), 636(s), 583(s), 558(s), and 453(w).

$Co_4(\mu_3\text{-}O)_4(\mu\text{-}O_2CMe)_4(py)_4$ (1a). Complex **1a** without cocrystallizing salts or solvent molecules can be isolated at a higher yield by following this procedure. $Co(NO_3)_2\cdot 6H_2O$ (2.90 g, 10 mmol) and $CH_3CO_2Na\cdot 3H_2O$ (2.7 g, 20 mmol) are stirred in methanol (30 mL) and heated to refluxing temperature, and pyridine (0.08 mL, 10 mmol) is added to the stirred reaction mixture. A portion of 30% hydrogen peroxide (v/v, 5 mL, ~50 mmol) is slowly added to the reaction mixture, and stirring under refluxing condition is continued for 4 h. The cooled reaction mixture is concentrated in a rotary evaporator, and then the aqueous layer is separated out by adding dichloromethane to it. The light-pink aqueous layer is discarded, and the CH_2Cl_2 layer is dried over anhydrous Na_2SO_4. An olive-green compound precipitates on adding petroleum ether to the dichloromethane solution. The product is dried in a vacuum desiccator over fused $CaCl_2$. Yield: 1.59 g (74% based on cobalt). The dried sample was analyzed as **1a**. Anal. Calcd for $C_{28}H_{32}N_4O_{12}Co_4$: C, 39.46; H, 3.78; N, 6.57: Co, 27.65. Found: C, 39.68; H, 4.08; N, 6.31; Co, 27.21 (gravimetric). IR data (KBr pellet, ν_{max}/cm^{-1}) for **1a**: 3400(w, br), 3109(w), 3073(w), 2925(w), 1607(m), 1538(vs), 1483(s), 1449(s), 1410(vs), 1385(vs), 1339(w), 1211(m), 1153(m), 1071(m), 1045(w), 1019(w), 763(s), 696(s), 634(s), 583(s), and 454(w).

Analogous procedures have also been adopted to obtain compounds **1b**−**d**.

$Co_4(\mu_3\text{-}O)_4(\mu\text{-}O_2CMe)_4(4\text{-}Mepy)_4$ (1b). Stirring of $Co(NO_3)_2\cdot 6H_2O$ (2.90 g, 10 mmol) and $CH_3CO_2Na\cdot 3H_2O$ (2.7 g, 20 mmol) in methanol (30 mL) results in a pink solution. The addition of 4-methylpyridine (0.98 mL, 10 mmol) to the refluxed reaction mixture changes the color to red from pink. A portion of 30% hydrogen peroxide (v/v, 5 mL, ~50 mmol) is then slowly added to the reaction mixture, and stirring under refluxing condition is continued for 4 h. The volume of the reaction mixture is reduced, and the procedure given above for **1a** is followed to obtain an olive-green product. Yield: 1.51 g (67% based on cobalt). The dried sample was analyzed as **1b**. Anal. Calcd for $C_{32}H_{40}N_4O_{12}Co_4$: C, 42.31; H, 4.44; N, 6.17. Found: C, 42.01; H, 4.62; N, 6.34. IR data (KBr pellet, ν_{max}/cm^{-1}): 3447(s, br), 3080(w), 2925(w), 1654(w), 1622(s), 1582(w), 1538(vs), 1502(s), 1412(s), 1385(vs), 1338(w), 1208(s), 1169(m), 1037(m), 813(m), 718(w), 698(m), 634(s), and 584(m).

$Co_4(\mu_3\text{-}O)_4(\mu\text{-}O_2CMe)_4(4\text{-}Etpy)_4$ (1c). $Co(NO_3)_2\cdot 6H_2O$ (2.90 g, 10 mmol), $CH_3CO_2Na\cdot 3H_2O$ (2.7 g, 20 mmol), and 4-ethylpyridine (1.13 mL, 10 mmol) are stirred in refluxing methanol (30 mL), and the procedure described above for the synthesis of **1a** and **1b** is followed thereafter to obtain the product as an olive-green powder. Yield: 1.52 g (63% based on cobalt). The dried sample was analyzed as **1c**. Anal. Calcd for $C_{36}H_{48}N_4O_{12}Co_4$: C, 44.83; H, 5.02; N, 5.81. Found: C, 44.97; H, 4.40; N, 5.98. IR data (KBr pellet, ν_{max}/cm^{-1}): 3423(s, br), 3083(w), 2970(m), 2934(w), 2877(w), 1621(s), 1535(vs), 1504(s), 1409(vs), 1386(vs), 1344(m), 1220(m), 1067(m), 1036(m), 833(s), 793(m), 700(s), 635(s), 584(s), and 522(w).

$Co_4(\mu_3\text{-}O)_4(\mu\text{-}O_2CMe)_4(4\text{-}CNpy)_4$ (1d). Preparation of this compound using the above general procedure leads to 52% product yield.[12] C, H, N, and Co analyses match well with the composition. An olive-green powder of identical composition and spectral behavior may also be isolated at a reduced yield (42%) directly as a precipitate from the concentrated reaction mixture obtained prior to CH_2Cl_2 extraction. IR data (KBr pellet, ν_{max}/cm^{-1}): 3569(w), 3535(w), 3428(w), 3218(w), 3116(w), 3055(w), 3012(w), 2931(w), 2250(m), 1611(m), 1533(vs), 1492(s), 1411(vs), 1338(s), 1219(s), 1065(m), 1030(w), 831(s), 791(m), 698(s), 634(s), 579(s), and 558(m).

X-ray Crystallographic Studies. The intensity data for **1a** and **1b** were collected on Bruker CCD diffractometers using the *SMART/SAINT* software.[16] Suitable crystals were picked for X-ray crystallographic work by microscopic examination. Intensity data were collected using graphite-monochromatized Mo Kα radiation (λ = 0.7107 Å) at 293 K. The chosen crystals were found to be stable against thermal decomposition and radiation-induced decay.

The structures were solved by direct methods (*SHELXS-97*) and standard Fourier techniques and refined on F^2 using full matrix

(16) *SMART/SAINT*; Bruker AXS, Inc.: Madison, WI, 2004.

Table 1. Crystallographic Data for **1a** and **1b**

	1a·$NaClO_4$·$3.5H_2O$	**1a**·$0.5NaNO_3$·$8H_2O$[13]	**1a**·$5CHCl_3$[3]	**1b**·$3H_2O$
formula	$C_{28}H_{32}N_4O_{12}Co_4$·$NaClO_4$·$3.5H_2O$	$C_{28}H_{32}N_4O_{12}Co_4$·$0.5NaNO_3$·$8H_2O$	$C_{28}H_{32}N_4O_{12}Co_4$·$5CHCl_3$	$C_{32}H_{40}N_4O_{12}Co_4$·$3H_2O$
M	1037.22	1026.83	1446.18	961.72
system, space group	tetragonal, $I\bar{4}2d$	triclinic, $P\bar{1}$ (No. 2)	orthorhombic, *Pnma*	orthorhombic, *Pnnm*
a/Å	12.398(4)	10.122(1)	10.181(4)	16.733(2)
b/Å	12.398(4)	11.177(1)	21.665(2)	17.510(2)
c/Å	53.97(2)	36.620(4)	27.407(6)	13.190(2)
α/deg	90	92.187(2)	90	90
β/deg	90	91.111(2)	90	90
γ/deg	90	103.145(2)	90	90
V/Å^3	8295(5)	4029.8(7)	6043(2)	3864.7(9)
Z	8	4	4	4
T/K	293	100		293
λ/Å	0.71073	0.71073		0.71073
D_{calc}/g cm^{-3}	1.641	1.692	1.590	1.561
μ/mm^{-1}	1.725	1.710		1.749
$R(F_o)$[a]	0.0394/0.0384 for 3684 unique and 3575 observed reflections; l.s. parameters = 261	0.1361/0.1072 for 15 780 unique and 12 046 observed reflections; l.s. parameters = 1083	0.087[b]	0.1548/0.0824 for 3684 unique and 2569 observed reflections; l.s. parameters = 270
$R_w(F_o^2)$	0.1238/0.1225	0.2162/0.2063	0.084[b]	0.2504/0.1986

[a] R and R_w values are for all unique data and the observed data with $F_o \geq 4\sigma(F_o)$; $R = \sum||F_o| - |F_c||\sum|F_o|$; $R_w = \{\sum[w(F_o^2 - F_c^2)^2]/\sum[w(F_o^2)^2]\}^{1/2}$ where $w = 1/[\sigma^2(F_o^2) + (aP)^2 + bP]$ with P is $[2F_c^2 + \max(F_o^2,0)]/3$. [b] Per ref 3.

least-squares procedures (*SHELXL-97*) using the *SHELX-97* package[17] incorporated in *WinGX*.[18] Empirical absorption corrections were applied with *SADABS*.[19] Structural illustrations were drawn using either *ORTEP-3* for Windows[20] or *PLUTON*.[21]

Crystal Structure of 1a·$NaClO_4$·$3.5H_2O$. The tetragonal crystal system for **1a**·$NaClO_4$·$3.5H_2O$ was established by routine procedures. The choice of the noncentrosymmetric space group $I\bar{4}2d$ (No. 122) was confirmed by the successful solution and refinement of the structure. All non-hydrogen atoms were refined anisotropically except for the OW2 and OW3 atoms for the water molecules, which are in a disordered state. Hydrogen atoms were assigned idealized positions and given thermal parameters equivalent to either 1.5 (methyl hydrogen atoms) or 1.2 (pyridine-ring hydrogen atoms) times the thermal parameter of the carbon atoms to which they were attached. The disordered region of electron density in the difference Fourier map was modeled as partially occupied (0.5 for O2W and 0.25 for O2W) water molecules. Hydrogen atoms of the water molecules were not found. Crystallographic data on **1a**·$NaClO_4$·$3.5H_2O$ are given in Table 1.

Crystal Structure of 1b·$3H_2O$. The dark-green prismatic crystal of **1b**·$3H_2O$ used for X-ray crystallographic study was obtained from the concentrated reaction mixture. All non-hydrogen atoms were refined anisotropically except for OW3 and OW4, which were found to be disordered and hence refined with partial site-occupation fraction values of 0.25 that gave reasonable U_{11} values. For the water molecules, the hydrogen atoms were not located. A few relatively strong electron density peaks (which are believed to be an artifact of measurement and/or absorption correction) near the cobalt atoms were not included in structure-factor calculations. Relevant crystallographic data are given in Table 1.

Oxidation of Ethylbenzene. The oxidation of ethylbenzene was performed in a glass vessel fitted with an overhead stirrer under atmospheric pressure. Air was used as oxidant at a flow rate of 0.4 L/min. A portion of 0.25 g of complex **1a** was suspended in neat ethylbenzene (150 mL, 1.25 mol), and the stirred reaction mixture was heated to 120 °C. The reaction was carried out for 24 h. Both the evaporating substrate and reaction byproduct water were collected in a Dean−Stark trap, and the overflowing ethylbenzene continuously replenished the reacting substrate. The reaction was monitored by GC, and products were identified by comparing them with authentic samples.

Oxidation of *p*-Xylene. The oxidation of *p*-xylene was carried out in the following manner. Complex **1a** (0.1 g) was suspended in the neat substrate (30 mL) taken in a round-bottomed flask fitted with a magnetic pellet and an air inlet. The flask was heated to 130 °C, and air was bubbled through the rapidly stirred solution. The water formed during the course of the reaction was collected using a Dean−Stark trap, on top of which a condenser was fitted to minimize the loss of evaporating substrate by circulating cooled water through the condenser. Oxidized product accumulated as a white solid, and the reaction was stopped after about 7 h when stirring of the reaction mixture was no longer possible due to the buildup of a large amount of solid product. The solid product is filtered off, and the residue is treated with ethanol, in which *p*-toluic acid is highly soluble whereas terephthalic acid does not have any appreciable solubility. Isolated yield: *p*-methyl benzoic acid, 8.2 g (~25%) and terephthalic acid, 0.39 g (~1%).

Results and Discussion

Synthesis of μ_3-Oxo Cobalt(III) Acetate Clusters Having the Co_4O_4 Core. Syntheses of Co(III) complexes are generally achieved by the aerobic or chemical oxidation of

(17) Sheldrick, G. M. *SHELX-97, Program for the Solution and Refinement of Crystal Structures*; University of Göttingen, Göttingen, Germany, 1998.
(18) Farrugia, L. J. *WinGX: An Integrated System of Windows Programs for the Solution, Refinement and Analysis for Single Crystal X-ray Diffraction Data*, version 1.65.04; Department of Chemistry: University of Glasgow, 2003. (Farrugia, L. J. *J. Appl. Crystallogr.* **1999**, *32*, 837−838).
(19) Sheldrick, G. M. *SADABS, Bruker Nonius Area Detector Scaling and Absorption Correction*, version 2.05; University of Göttingen, Göttingen, Germany, 1999.
(20) (a) Burnett, M. N.; Johnson, C. K. *ORTEP-III, Oak Ridge Thermal Ellipsoid Plot for Crystal Structure Illustrations*; Report ORNL-6895; Oak Ridge National Laboratory: Oak Ridge, TN, 1996. (b) Farrugia, L. J. *ORTEP-3* for Windows, version 1.08. *J. Appl. Crystallogr.* **1997**, *30*, 565.
(21) Spek, A. L. *Acta Crystallogr.* **1990**, *A46*, C34.

Scheme 1

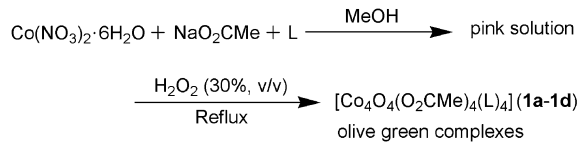

Co(II) salts in the presence of appropriate ligands. Such transformations often proceed through Co(III)−superoxo or binuclear μ-peroxo intermediates.[22] The synthetic strategy for the preparation of the complexes **1a**−**d** in the present study is summarized in Scheme 1. The process involves the reaction of cobalt nitrate hexahydrate, $Co(NO_3)_2 \cdot 6H_2O$, with 2 equiv of NaO_2CMe and 1 equiv of N-donor ligands, pyridine, 4-methylpyridine, 4-ethylpyridine, and 4-cyanopyridine (L) in methanol. Oxidation of the resulting cobalt(II) solution under refluxing conditions for 4 h with excess H_2O_2 leads to an olive-green solution from which the dark-olive-green complexes $Co_4O_4(O_2CMe)_4(L)_4$ (**1a**−**d**) are isolated.

In the above scheme, L = py, 4-Mepy, 4-Etpy, and 4-CNpy, respectively, denote the complexes, called **1a**, **1b**, **1c**, and **1d**, that can be obtained as precipitates from the concentrated reaction solution. However, the isolated yields of the products are relatively low due to their solubility in the solvent system used. But isolation via precipitation upon the addition of petroleum ether to a CH_2Cl_2 extract of the reaction mixture leads to a higher yield without affecting the purity of the products. All four complexes prepared by this general route have been subjected to most of the physicochemical studies.

Beattie et al. isolated[3] the complex $Co_4O_4(O_2CMe)_4(py)_4$ from a mixture of several di- and trinuclear complexes in low yield. These synthetic procedures require at least two steps to prepare the cubane complexes from simple cobalt(II) salts. In contrast, the synthetic method developed by us is rather simple because in all cases we are able to use $Co(NO_3)_2 \cdot 6H_2O$ in MeOH as the starting material and the H_2O_2 oxidation of Co(II) in the presence of NaO_2CMe and the required pyridine or substituted pyridine ligand for the successful preparation of the cluster complexes. This makes our procedure quite general for the synthesis of cubane-like tetrameric cobalt(III) complexes of the type $Co_4O_4(O_2CMe)_4(py)_4$. Yields obtained for the complexes are moderate to high. The significant aspect of our work is the absence of complexes of other nuclearities, which were commonly observed by other authors.[2,3] Also, while using a dichloromethane extract of the olive-green products during the workup procedure for isolating the complexes in improved yields, the complexes were invariably found to be identical to the complex species present in the precipitated products obtained directly from the reaction mixtures. The presence of dinuclear and/or trinuclear complexes can be ruled out by examining the infrared spectra of the isolated products. Furthermore, electrochemical investigations (vide infra) have corroborated these findings. It is, however, pertinent to note here that the discarded solutions in our isolation of the cubane clusters may contain cobalt(II) species, which have not been identified.

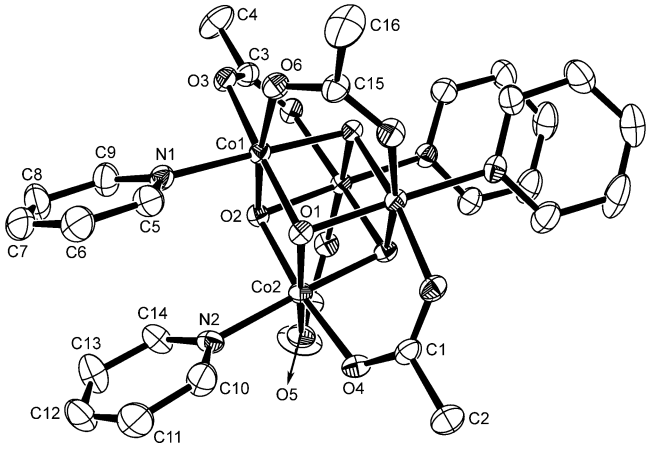

Figure 1. Labeled *ORTEP* (30% probability) representation of complex **1a** in **1a**·$NaClO_4 \cdot 3.5H_2O$. Hydrogen atoms are omitted for clarity.

The complexes **1** are soluble in common organic solvents to varying degrees. While they readily dissolve in water, their solubility is rather low in chloroform. As described earlier,[13] complex **1a** dissolves in several solvents of widely differing polarity. That the integrity of the complex remains intact in solution can be judged from the striking similarity of the visible spectra of the resulting solutions, notwithstanding some red/blue shifts in the absorption maxima (vide infra). Since the crystalline product obtained directly from the reaction mixture gives an electrically conductive solution in water, it was initially believed that there could be cationic complexes present in this solution. With a view to isolating the perchlorate salt of the species present in aqueous medium, $NaClO_4$ was added to the solution. However, as will be presently seen, although the aqueous solution of **1a** is electrically conductive, the species isolated as the product in such a manner has the composition **1a**·$NaClO_4 \cdot 3.5H_2O$. It is also possible to obtain a crystalline species having the composition **1a**·$KPF_6 \cdot 3H_2O$ by using KPF_6 in place of $NaClO_4$. Indeed, the rod-shaped crystals obtained directly from the reaction mixture following the partial removal of solvent also contain the cubane tetramer associated with a cocrystallizing alkali-metal salt. This crystalline species has the composition **1a**·$NaNO_3 \cdot 8H_2O$.[13] These facts, coupled with our inability to obtain a crystalline sample of $Co_4O_4(O_2CMe)_4(py)_4$, alone appear to suggest the role of cocrystallizing salts in the formation of crystals via a supramolecular mechanism (vide infra). As discussed below, evidence regarding the presence of the salts in the crystalline samples of $Co_4O_4(O_2CMe)_4(py)_4$ is obtainable from their infrared spectra.

Structure of $Co_4(\mu_3\text{-}O)_4(\mu\text{-}O_2CMe)_4(py)_4$ (1a). The composition of rodlike crystals obtained directly from the preparative reaction mixture was earlier established as **1a**·$0.5NaNO_3 \cdot 8H_2O$.[13] On the other hand, dark-olive-green crystals of composition **1a**·$NaClO_4 \cdot 3.5H_2O$ are obtained in rectangular blocklike morphology from the concentrated reaction mixture containing aqueous $NaClO_4$. Crystal data on **1a**·$NaClO_4 \cdot 3.5H_2O$ are presented along with those for **1a**·$0.5NaNO_3 \cdot 8H_2O$ in Table 1, which also includes com-

(22) Cotton, F. A.; Willkinson, G. *Advanced Inorganic Chemistry*, 5th ed.; Wiley: New York, 1988; pp. 735−738.

Table 2. Selected Interatomic Distances (Å) and Angles (deg) for **1a**·$NaClO_4$·3.5H_2O and **1a**·0.5$NaNO_3$·8H_2O

		1a·$NaClO_4$·3.5H_2O	
Co(1)−Co(2)#1[a]	2.705(1)	Co(1)−Co(1)#1[a]	2.708(1)
Co(1)−Co(2)	2.823(1)	Co(2)−Co(2)#1[a]	2.718(1)
Co(1)−O(1)	1.872(2)	Co(1)−O(2)	1.860(3)
Co(1)−O(3)	1.962(3)	Co(1)−O(6)	1.951(3)
Co(1)−N(1)	1.956(4)	Co(1)−Co(2)	2.823(1)
Co(2)−O(1)	1.871(3)	Co(2)−O(2)	1.869(2)
Co(2)−O(4)	1.948(3)	Co(2)−O(5)	1.962(3)
Co(2)−N(2)	1.971(4)	O(3)−Na(1)	2.538(4)
O(6)−Na(1)	2.648(3)	Na(1)−O(1W)	2.325(5)
Cl(1)−O(7)	1.366(6)	Cl(1)−O(8)	1.710(7)
Co(2)#1−Co(1)−Co(1)#1[a]	62.8(2)	Co(2)#1−Co(1)−Co(2)[a]	58.8(3)
Co(1)#1−Co(1)−Co(2)[a]	58.5(2)	Co(1)#1−Co(2)−Co(2)#1[a]	62.7(2)
O(2)−Co(1)−O(1)	81.9(1)	O(2)−Co(1)−O(6)	172.3(1)
O(1)−Co(1)−O(6)	92.7(1)	O(2)−Co(1)−N(1)	94.4(1)
O(1)−Co(1)−N(1)	91.5(1)	O(6)−Co(1)−N(1)	91.2(1)
O(2)−Co(1)−O(3)	90.2(1)	O(1)−Co(1)−O(3)	170.9(1)
O(6)−Co(1)−O(3)	94.6(1)	N(1)−Co(1)−O(3)	93.5(1)
O(2)−Co(1)−Na(1)	136.1(8)	O(1)−Co(1)−Na(1)	141.9(8)
O(6)−Co(1)−Na(1)	49.2(1)	N(1)−Co(1)−Na(1)	87.6(1)
O(3)−Co(1)−Na(1)	45.9(1)	O(2)−Co(2)−O(1)	81.7(1)
O(2)−Co(2)−O(4)	170.5(1)	O(1)−Co(2)−O(4)	90.5(1)
O(2)−Co(2)−O(5)	89.6(1)	O(1)−Co(2)−O(5)	169.9(1)
O(4)−Co(2)−O(5)	97.6(1)	O(2)−Co(2)−N(2)	95.3(1)
O(1)−Co(2)−N(2)	94.9(1)	O(4)−Co(2)−N(2)	90.7(1)
O(5)−Co(2)−N(2)	90.9(1)	Co(2)−O(1)−Co(1)	97.9(1)
Co(1)−O(2)−Co(2)	98.4(1)	Co(1)−O(3)−Na(1)	100.2(1)
Co(1)−O(6)−Na(1)	96.9(1)	O(1W)−Na(1)−O(3)	176.8(2)
O(1W)−Na(1)−O(6)	109.5(2)	O(3)−Na(1)−O(6)	67.3(9)
O(1W)−Na(1)−Co(1)	143.1(2)	O(7)−Cl(1)−O(8)	102.7(5)
		1a·0.5$NaNO_3$·8H_2O	
Co(1)−Co(3)	2.699(2)	Co(1)−Co(4)	2.701(2)
Co(1)−Co(2)	2.806(2)	Co(2)−Co(4)	2.696(2)
Co(2)−Co(3)	2.710(2)	Co(3)−Co(4)	2.824(2)
Co(5)−Co(7)	2.699(2)	Co(5)−Co(8)	2.712(2)
Co(5)−Co(6)	2.825(2)	Co(6)−Co(7)	2.703(2)
Co(6)−Co(8)	2.711(2)	Co(7)−Co(8)	2.825(2)
Co(1)−O(2)	1.843(6)	Co(1)−O(1)	1.866(6)
Co(1)−O(3)	1.885(6)	Co(1)−O(5)	1.947(6)
Co(1)−N(1)	1.949(7)	Co(1)−O(11)	1.950(6)
Co(2)−O(2)	1.862(6)	Co(2)−O(4)	1.863(6)
Co(2)−O(1)	1.865(7)	Co(2)−O(10)	1.947(6)
Co(2)−N(2)	1.959(8)	Co(2)−O(7)	1.962(6)
Co(3)−O(4)	1.855(6)	Co(3)−O(1)	1.871(6)
Co(3)−O(3)	1.871(6)	Co(3)−O(9)	1.942(6)
Co(3)−N(3)	1.971(7)	Co(3)−O(6)	1.982(6)
Co(4)−O(4)	1.850(6)	Co(4)−O(2)	1.866(6)
Co(4)−O(3)	1.877(7)	Co(4)−O(8)	1.928(7)
Co(4)−O(12)	1.965(6)	Co(4)−N(4)	1.968(7)
Co(5)−O(13)	1.868(6)	Na(1)−O(11)	2.362(8)
Na(1)−O(5)	2.379(7)	Na(1)−O(2S)	2.263(8)
Na(1)−O(1S)	2.266(9)	Na(1)−O(3S)	2.400(8)
Co(3)−Co(1)−Co(4)	63.04(4)	Co(3)−Co(1)−Co(2)	58.95(4)
Co(4)−Co(1)−Co(2)	58.58(4)	Co(4)−Co(2)−Co(3)	62.97(4)
Co(4)−Co(2)−Co(1)	58.78(4)	Co(3)−Co(2)−Co(1)	58.56(4)
Co(1)−Co(3)−Co(2)	62.48(4)	Co(1)−Co(3)−Co(4)	58.52(4)
Co(2)−Co(3)−Co(4)	58.26(4)	Co(2)−Co(4)−Co(3)	58.77(4)
Co(1)−Co(4)−Co(3)	58.44(4)	Co(7)−Co(5)−Co(6)	58.55(5)
Co(8)−Co(5)−Co(6)	58.60(5)	Co(7)−Co(6)−Co(8)	62.90(5)
Co(7)−Co(6)−Co(5)	58.41(5)	Co(8)−Co(6)−Co(5)	58.63(5)
Co(5)−Co(7)−Co(8)	58.76(5)	Co(6)−Co(7)−Co(8)	58.70(5)
Co(6)−Co(8)−Co(5)	62.77(5)	Co(6)−Co(8)−Co(7)	58.41(5)
Co(5)−Co(8)−Co(7)	58.30(5)	O(2)−Co(1)−O(1)	82.2(3)
O(2)−Co(1)−O(3)	87.1(3)	O(1)−Co(1)−O(3)	87.1(3)
O(2)−Co(1)−O(5)	172.1(3)	O(1)−Co(1)−O(5)	90.9(3)
O(3)−Co(1)−O(5)	88.7(3)	O(2)−Co(1)−N(1)	93.9(3)
O(1)−Co(1)−N(1)	94.9(3)	O(3)−Co(1)−N(1)	177.9(3)
O(5)−Co(1)−N(1)	90.6(3)	O(2)−Co(1)−O(11)	91.1(3)
O(1)−Co(1)−O(11)	171.4(3)	O(3)−Co(1)−O(11)	87.2(3)
O(5)−Co(1)−O(11)	95.4(3)	N(1)−Co(1)−O(11)	90.9(3)
Co(1)−O(5)−Na(1)	94.6(3)	Co(1)−O(11)−Na(1)	95.0(3)
O(2S)−Na(1)−O(1S)	93.8(3)	O(2S)−Na(1)−O(11)	91.9(3)
O(1S)−Na(1)−O(11)	168.7(3)	O(2S)−Na(1)−O(5)	126.3(3)
O(1S)−Na(1)−O(5)	109.3(3)	O(11)−Na(1)−O(5)	74.9(2)
O(2S)−Na(1)−O(3S)	146.8(3)	O(1S)−Na(1)−O(3S)	92.6(3)
O(11)−Na(1)−O(3S)	77.4(3)	O(5)−Na(1)−O(3S)	81.6(3)

[a] Symmetry code #1: $-x+1, -y-1, z$.

parable data on the previously[3] determined crystal structure of compound **1a**. A labeled *ORTEP* diagram of $[Co_4O_4(O_2CMe)_4(py)_4]$ in **1a**·$NaClO_4$·3.5H_2O is shown in Figure 1, and selected interatomic distances and angles are listed in Table 2.

The compound **1a**·$NaClO_4$·3.5H_2O crystallizes in an acentric tetragonal space group $I\bar{4}2d$ with one-half a formula unit included in the asymmetric unit, which is related to the other half by a two-fold axis running through the C−C bonds of two acetato ligands that bridge the Co···Co diagonals on a pair of opposite faces of the Co_4O_4 cube. Each cubane-like molecule consists of four each of Co^{3+} and O^{2-} ions present at alternate corners of an approximate cube to form a cubane-like $[Co_4O_4]^{4+}$ core with acetato ligands bridging the Co^{3+} ions along four face diagonals of the cube. Pyridine ligands occupy the most outlying sites on the octahedral Co(III) centers. All four cobalt atoms are thus in the +3 oxidation state and as expected for d^6-Co^{3+} ions, the metal centers adopt nearly octahedral six-coordinate geometries.

Inspection of the structural parameters leads to the conclusion that for the Co^{III} ions, the Co^{III}−O(oxide) and Co^{III}−O(carboxylate) bond lengths are in the fairly narrow ranges of 1.860(3)−1.876(3) and 1.948(3)−1.962(3) Å, respectively. These values are consistent with a low-spin configuration of Co(III). The average Co−N distance is of the order of 1.96 Å. Two types of Co···Co distances, close to (i) 2.82 Å when Co···Co is bridged by two oxo ligands only, and (ii) 2.70 Å when bridged by two oxo ligands and a bidentate carboxylato ligand, are observed. Similar distances were also observed for related cobalt(III) complexes having a "$Co_4(\mu_3\text{-}O)_4$" arrangement (vide infra).[2−4]

An interesting feature of the crystal structure of **1a**·$NaClO_4$·3.5H_2O is the presence of Na^+ ions in an approximately octahedral environment surrounded by six oxygen atoms, four from two carboxyl groups and the other two from two H_2O molecules of crystallization (Figure 2). The Na−O(aqua) distances are short, 2.325(5) Å, while the Na−O(carboxyl) bonds are considerably longer, O3−Na1 = 2.538(4) Å and O6−Na1 = 2.648(3) Å, which are consistent with previously reported values.[23] The presence of Na^+ at a bridging position thus joins the tetrameric complexes into zigzag chains that run along the crystallographic *a* and *b* directions. The two chains are related by $\bar{4}$ symmetry. Several weak hydrogen bonds appear to play a significant role in the crystal structure. Clearly, supramolecular interactions are highly important in the stabilization of the crystal structure of **1a**·$NaClO_4$·3.5H_2O.

In the crystal structure of **1a**·0.5$NaNO_3$·8H_2O,[13] 2 molecules of the tetramer $[Co_4(\mu_3\text{-}O)_4(\mu\text{-}O_2CMe)_4(py)_4]$ along with 1 formula unit of $NaNO_3$ and 16 H_2O molecules are

(23) (a) Korpar-Čolig, B.; Cindrić, M.; Matković-Čalogović, D.; Vrdoljak, V.; Kamenar, B. *Polyhedron* **2002**, *21*, 147−153. (b) Miyasaka, H.; Kachi-Terajima, C.; Ishii, T.; Yamashita, M. *J. Chem. Soc., Dalton Trans.* **2001**, 1929−1930. (c) Berchin, E. K.; Graham, A.; Parkin, A.; Parsons, S.; Seddon, A. M.; Winpenny, R. E. P. *J. Chem. Soc., Dalton Trans.* **2000**, 3242−3252. (d) Price, D. J.; Powell, A. K.; Wood, P. T. *J. Chem. Soc., Dalton Trans.* **2000**, 3566−3569. (e) Sakagami, N.; Kita, E.; Kita, P.; Wisniewska, J.; Kaizaki, S. *Polyhedron* **1999**, *18*, 2001−2007.

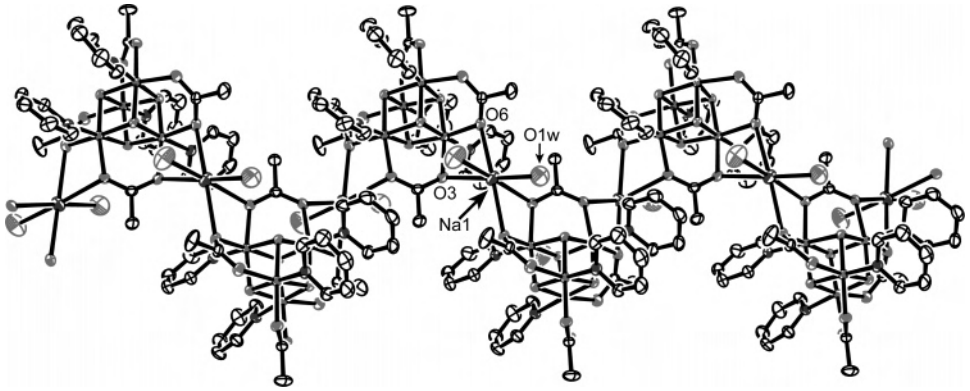

Figure 2. Octahedrally coordinated Na atoms linking cubane complexes containing $[Co_4(\mu_3\text{-}O)_4]^{4+}$ cores into a zigzag supramolecular chain in **1a**·$NaClO_4$·$3.5H_2O$. Hydrogen atoms and uncoordinated water molecules are omitted for clarity.

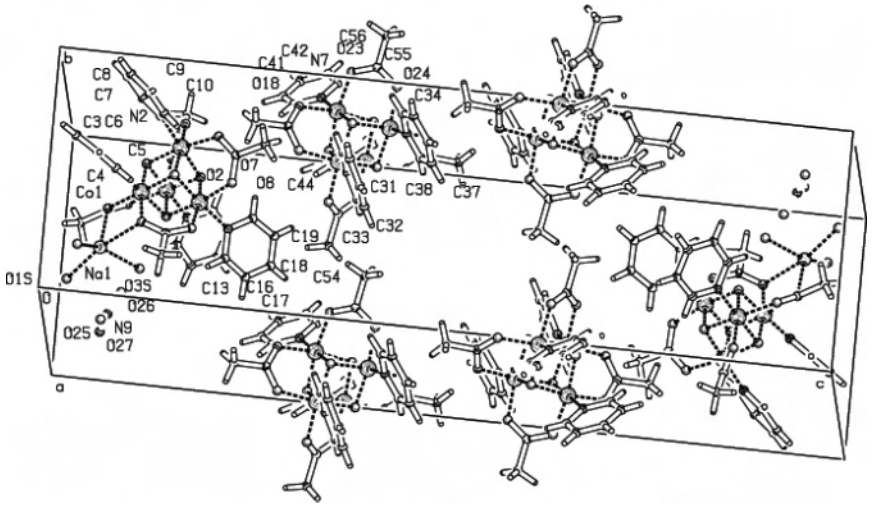

Figure 3. Unit cell packing diagram for **1a**·$0.5NaNO_3$·$8H_2O$ with omission of the uncoordinated water molecules on grounds of clarity. All atoms in the crystal structure occupy general positions. Nine of the water molecules of crystallization are of full occupancy, while the remaining seven are in a highly disordered state. Most of the oxygen atoms in the coordinated and uncoordinated water molecules are found at positions close enough for hydrogen-bonding interactions with oxygen atoms in the carboxylate and nitrate anions. The uncoordinated water molecules appear to occupy intermolecular space in channel-like formations aided by hydrogen bonds.

found to constitute the asymmetric unit of the triclinic unit cell (Figure 3). Although the crystals are indefinitely stable at room temperature, the water molecules may be induced to leave the crystal lattice irreversibly at 128 °C as shown by thermogravimetric studies.[13]

Crystal Structure of $Co_4(\mu_3\text{-}O)_4(\mu\text{-}O_2CMe)_4(4\text{-}Mepy)_4$ (1b). Dark-green crystals of **1b** were obtained by storing the concentrated reaction mixture for several days. The crystal structure of this compound having a composition **1b**·$3H_2O$ has been determined (Table 1). The molecular structure of **1b** is shown in Figure 4. Selected geometric parameters are listed in Table 3.

As in the case of **1a**, the structure of complex **1b** also consists of a central $[Co_4(\mu_3\text{-}O)_4]^{4+}$ cubane-like core. Two of the three cobalt atoms, Co2 and Co3 in the asymmetric unit, lie on a mirror plane containing eight other atoms of O1, O3, N2, N3, C13, C14, C17, and C18 (at *x*, *y*, 0), which bisects the Co1···Co1′ (*x*, *y*, 0) vector. The overall molecular structure as well as the octahedral coordination geometry around each Co(III) center are analogous to that of **1a** with peripheral ligation for each metal provided by three oxo anions, the pyridyl-N atom of 4-methylpyridine, and two carboxyl oxygen atoms from two carboxylato ligands, which

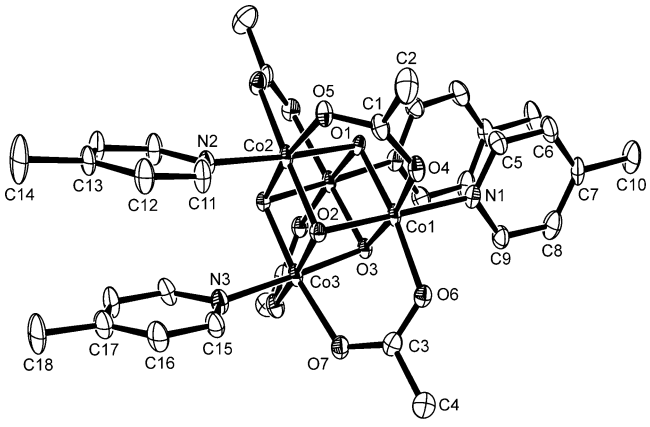

Figure 4. Labeled *ORTEP* (30% probability) representation of the complex $Co_4(\mu_3\text{-}O)_4(\mu\text{-}O_2CMe)_4(4\text{-}Mepy)_4$ in **1b**·$3H_2O$. Hydrogen atoms and water molecules are omitted for clarity.

bridge the cobalt atoms pairwise in the familiar syn−syn manner. The Co_4O_4 cube deviates considerably from ideal geometry. The internal cube angles (O−Co−O) at the metal vertices average at 85.27°, whereas the comparable angles at the oxo vertices (Co−O−Co) are much larger, averaging 94.31°, to keep the bulky Co(III) complexes as far apart as possible. Two types of Co−O bonds for each cobalt center

Table 3. Selected Interatomic Distances (Å) and Angles for **1b**·$3H_2O$

Co(1)−O(2)	1.857(4)	Co(1)−O(3)	1.873(4)
Co(1)−O(1)	1.883(4)	Co(1)−O(6)	1.950(4)
Co(1)−O(4)	1.958(5)	Co(1)−N(1)	1.961(6)
Co(1)−Co(3)	2.695(1)	Co(1)−Co(2)	2.707(1)
Co(2)−O(2)	1.860(4)	Co(2)−O(1)	1.865(5)
Co(2)−O(5)	1.965(5)	Co(2)−N(2)	1.972(7)
Co(2)−Co(3)	2.813(2)	Co(3)−O(3)	1.851(6)
Co(3)−O(2)	1.872(4)	Co(3)−N(3)	1.944(8)
Co(3)−O(7)	1.969(5)		
O(2)−Co(1)−O(3)	86.7(2)	O(2)−Co(1)−O(1)	86.3(2)
O(3)−Co(1)−O(1)	82.7(2)	O(2)−Co(1)−O(6)	89.2(2)
O(3)−Co(1)−O(6)	89.9(2)	O(1)−Co(1)−O(6)	171.6(2)
O(2)−Co(1)−O(4)	88.7(2)	O(3)−Co(1)−O(4)	171.5(2)
O(1)−Co(1)−O(4)	89.8(2)	O(6)−Co(1)−O(4)	97.2(2)
O(2)−Co(1)−N(1)	179.0(2)	O(3)−Co(1)−N(1)	94.2(2)
O(1)−Co(1)−N(1)	93.5(2)	O(6)−Co(1)−N(1)	91.2(2)
O(4)−Co(1)−N(1)	90.3(2)	Co(3)−Co(1)−Co(2)	62.76(4)
O(2)−Co(2)−O(1)	86.8(2)	O(2)−Co(2)−O(5)	90.7(2)
O(1)−Co(2)−O(5)	87.3(2)	O(2)−Co(2)−N(2)	96.4(2)
O(1)−Co(2)−N(2)	175.8(3)	O(5)−Co(2)−N(2)	89.9(2)
Co(1)−Co(2)−Co(3)	58.40(4)	O(3)−Co(3)−O(2)	86.9(2)
O(3)−Co(3)−N(3)	178.1(3)	O(2)−Co(3)−N(3)	91.6(2)
O(3)−Co(3)−O(7)	87.8(2)	O(2)−Co(3)−O(7)	90.7(2)
N(3)−Co(3)−O(7)	93.4(2)	Co(1)−Co(3)−Co(2)	58.84(4)
Co(2)−O(1)−Co(1)	92.5(2)	Co(1)−O(2)−Co(2)	93.5(2)
Co(1)−O(2)−Co(3)	92.6(2)	Co(2)−O(2)−Co(3)	97.8(2)
Co(3)−O(3)−Co(1)	92.7(2)		

are also seen in this structure where Co−O(oxide) bonds are shorter than Co−O(carboxyl) bonds. As can be seen from Table 3, the differences brought about in the Co−N bond lengths by the 4-Mepy ligand in place of py are insignificant.

It is seen from the above results that the cubane-like $[Co_4O_4]^{4+}$ core present in **1a** and **1b** is essentially the same as those present in the related compounds, which were reported earlier.[2−4] Important structural parameters of the cubane tetramers of Co(III) are compared in Table 4. It is observed that the peripheral ligands have only a minor influence on the geometry of the tetrameric Co(III)−oxo core present in the complexes. The $[Co_4(\mu_3\text{-}O)_4]^{4+}$ cuboid allows for two kinds of shortened Co···Co separations of ca. 2.8 and ca. 2.7 Å. Although these $Co^{3+}\cdots Co^{3+}$ distances are fairly long for direct Co−Co bond formation, the existence of an approximately tetrahedral assembly of four cobalt atoms in each compound is notable. Each O^{2-} ligand may then be considered to cap a triangular face of the Co_4 tetrahedron.

Infrared Spectra. Ligation of the acetato and pyridine ligands to Co(III) in all four complexes of type $Co_4O_4(O_2CMe)_4L_4$ (**1a**−**d**) is evident from their IR spectra. In the IR spectra of the reported Co(III) complexes, it is possible to identify bands due to bridging acetate anions as well as for the N-donor ligands, viz., pyridine, 4-cyanopyridine, 4-methylpyridine, and 4-ethylpyridine, but unequivocal band assignments are difficult to make. While bands occurring in the 1530−1538 cm^{-1} range for the four complexes may be assigned to the ν_{asym}(COO) vibration, the corresponding ν_{sym}(COO) vibration cannot be identified with certainty. This is attributed to the fact that bands due to the stretching vibrations of the pyridine ring also occur in the same region. The spectra of the compounds **1a** (obtained by CH_2Cl_2 extraction), **1a**·$0.5NaNO_3$·$8H_2O$, **1a**·$NaClO_4$·$3.5H_2O$, and **1a**·KPF_6·$3H_2O$, in the 500−2000 cm^{-1} region are shown in Figure 5. As can be seen, the spectra are very similar apart from the expected differences due to the presence of NO_3^-, ClO_4^-, and PF_6^- anions in the last three compounds. The most characteristic feature of the IR spectra is the appearance of a four-band pattern observed at ∼760, ∼695, ∼635, and ∼580 cm^{-1}, which are observed for **1a** at 763, 696, 634, and 583 cm^{-1}. These bands at nearly the same energies and with comparable relative intensities also appear in the spectra of **1b**−**1d**. Thus, assuming that the 763 cm^{-1} band in **1a** is due to a pyridine ring-based vibration, it is possible to suggest that one or more of the three bands near 700, 635, and 580 cm^{-1} in compounds of type $Co_4O_4(O_2CMe)_4L_4$ are due to the "Co_4O_4" cubane-like core present in these compounds. The band at ∼635 cm^{-1} is tentatively assigned to a Co−O stretching vibration for $Co_3(\mu_3\text{-}O)$ group involving a tribridging oxo anion. This assumption is consistent with the determination of considerably shorter Co−O(oxo) bonds by X-ray diffraction (vide supra). Filled π orbitals on O^{2-} anions are likely to donate electrons to the electron-poor Co(III) centers to result in partial double-bond character of the Co(III)−O bonds. A band at a similar energy was earlier assigned[9b] to the $M_3(\mu_3\text{-}O)$ group, which commonly occurs in trinuclear oxo-centered complexes of type $M_3(\mu_3\text{-}O)(\mu\text{-}O_2CR)_6L_3]^{0/1+}$. Bands at comparable energies for the related $[Mn_4(\mu_3\text{-}O)_4]^{n+}$ complexes have also been ascribed to Mn−O vibrations.[24]

In view of the above observations, we believe that the infrared absorption bands near 700, 635, and 580 cm^{-1} can be used as a marker for the presence of cubane-like cobalt(III) oxo clusters having acetate anions as bridging ligands. This spectral analysis is of considerable practical importance in the characterization of supported reagents, which are useful as heterogeneous catalysts in the oxidation of several organic compounds.[11,13]

Electronic Spectra. The electronic spectral data obtained for the complexes **1a**−**d** are presented in Table 5. The spectra recorded for **1a** in CH_2Cl_2, MeOH, MeCN, and H_2O look very similar, but they are somewhat solvent- and concentration-dependent (Figure 6). The electronic spectra for **1a** in CH_2Cl_2 at three different concentrations are shown in Figure 6a. Three absorption bands are found to occur in the UV−vis region at 638 nm (sh), 362 nm (ϵ = 7428 M^{-1} cm^{-1}), and 227 nm (ϵ = 26 537 M^{-1} cm^{-1}). The lowest energy absorption appearing as a shoulder at 638 nm in CH_2Cl_2 is seen as moderately intense bands in MeOH, MeCN, and H_2O (Figure 6b) with ϵ values lying in the range of 300−400 M^{-1} cm^{-1}. Although the observed molar absorptivities are high for d−d transitions in centrosymmetric six-coordinate complexes, considering the distorted nature of the coordination spheres of Co^{3+} in **1a**, it is our belief that the absorption band being considered involves one of the two possible ligand-field transitions $^1A_1 \rightarrow {}^1T_1$ and $^1A_1 \rightarrow {}^1T_2$ for the approximately octahedral Co(III) complex. As judged from the observed intensities, the other two bands are attributable to sources other than ligand-field transitions. The first band at 362 nm is likely due to a charge-transfer transition

(24) Eppley, H. J.; Tsai, H.-L.; de Vries, N.; Folting, K.; Christou, G.; Hendrickson, D. N. *J. Am. Chem. Soc.* **1995**, *117*, 301−317.

Table 4. Average Interatomic Bond Distances (Å) and Angles (deg) for Tetranuclear Complexes Having the $[(Co^{III})_4(\mu_3\text{-}O)_4]^{4+}$ Core

compound[a]	Co−N_{arom}	Co-(μ_3-O)	Co−O_{carbox}	Co···Co[b]	Co···Co[c]	O−Co−O[d]	Co−O−Co[d]	ref
$[Co_4O_4(O_2CC_6H_4\text{-}p\text{-}Me)_2(bpy)_4](ClO_4)_2\cdot$ 2MeCN	1.939	1.882	1.959	2.852	2.665			2
$Co_4O_4(O_2CMe)_4(py)_4\cdot 5CHCl_3$	1.973	1.865	1.962	2.818	2.683	85.9	93.6	3
$Co_4(pg)_4O_4$	1.960	1.887	1.945	2.78		83.9	95.8	4
$Co_4O_4(O_2CMe)_4(py)_4\cdot 0.5NaNO_3\cdot 8H_2O$	1.962	1.865	1.953	2.815	2.702	85.0	94.6	13
$Co_4O_4(O_2CMe)_4(py)_4\cdot NaClO_4\cdot 3.5H_2O$	1.968	1.870	1.956	2.823	2.709	84.4	95.4	this work
$Co_4O_4(O_2CMe)_4\text{-}(4\text{-}Mepy)_4\cdot 3H_2O$	1.959	1.868	1.963	2.816	2.701	85.3	94.3	this work

[a] Hpg = *N*-(2-pyridylmethyl)glycine. [b] Bridged by two oxo ligands only. [c] Bridged by two oxo ligands and a bidentate carboxylato ligand. [d] Only oxygen atoms of the Co_4O_4 core are considered.

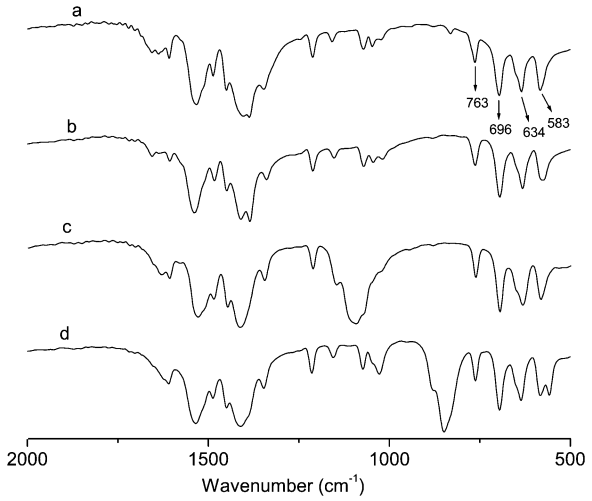

Figure 5. KBr phase infrared spectra of **1a**: (a) recrystallized from CH_2Cl_2 and petroleum ether mixture; (b) **1a**·$0.5NaNO_3\cdot 8H_2O$; (c) **1a**·$NaClO_4\cdot 3.5H_2O$; and (d) **1a**·$KPF_6\cdot 3H_2O$.

Table 5. Electronic Spectral Data on $Co_4(\mu_3\text{-}O)_4(\mu\text{-}O_2CMe)_4(L)_4$ (**1**) in Various Solvents

complex	solvent	electronic spectra: λ_{max}, nm (ϵ, M^{-1} cm^{-1})
1a	CH_2Cl_2	638 (sh), 362 (7428), 227 (26 537)
1a	MeOH	617 (360), 330 (5900), 246 (21 900)
1a	MeCN	650 (330), 355 (7149)
1a	H_2O	618 (388), 302 (sh), 350 (4,742), 257 (42 879)
1b	CH_2Cl_2	637 (sh), 354 (7935), 238 (sh)
1c	CH_2Cl_2	634 (sh), 353 (7825), 233 (35 710)
1d	CH_2Cl_2	634 (sh), 445 (8017), 362 (sh), 259 (22 500)

involving the μ_3-O−Co(III) moiety present in the complex. This band appears at 330 nm ($\epsilon = 5900$ M^{-1} cm^{-1}) and 355 nm ($\epsilon = 7149$ M^{-1} cm^{-1}) in MeOH and MeCN, respectively. The highest energy band at 227 nm is believed to be of ligand origin, most probably involving the $\pi \rightarrow \pi^*$ absorption of pyridine. This so-called $\pi \rightarrow$ p* band of pyridine itself appears at 257 nm. This assignment is supported by the observation of similar absorptions in CH_2Cl_2 for **1b**−**d** (Table 6) at similar energies. The presence of the substituted pyridine ligands also does not significantly alter the spectral behavior of the complexes. In all cases, the color of the CH_2Cl_2 solutions of the complexes is dark green, and as judged on the basis of persistent color and spectral examination, it may be added here that the complex species are stable in the dissolved state in dichoromethane. On the other hand, complex **1a** dissolves in water to produce a green-colored solution, which remains visibly and spectroscopically unchanged for about a day. However, prolonged storage of the solution leads to the slow reductive decomposition of $Co_4O_4(O_2CMe)_4(py)_4$ to produce unidentified cobalt(II) species.

A further notable point is that although the complexes $Co_4O_4(O_2CMe)_4L_4$ (**1a**−**d**) are neutral, they dissolve readily in water to give stable green solutions. The characteristic visible band due to the d−d transition remains similar in shape in the spectra recorded in H_2O, MeOH, and MeCN. While the visible band at 618 nm ($\epsilon = 388$ M^{-1} cm^{-1}) observed in H_2O occurs almost at the same energy with the band observed in MeOH (617 nm), the lower-energy LMCT bands in these two solvents appear at widely separated wavelengths (354 nm for H_2O and 330 nm for MeOH). Thus, the $[Co_4O_4]^{4+}$ core presumably undergoes deformation to varying degrees in different solvents. At the same time, the possibility of H_2O and MeOH entering into hydrogen-bonding interactions with the oxo ligands so as to distort the Co_4O_4 cube further also cannot be ruled out. This could perhaps explain why the d−d band positions in these two solvents appear at nearly the same energies; at the same time, it could also explain the λ_{max} value of 657 nm observed in MeCN. Similarities in the UV−vis spectra recorded for the four cluster compounds in these solvents are all close enough to suggest structural integrity of the complexes in solution.

NMR Spectra. ^{1}H NMR spectra recorded for the complexes **1a**−**d** are characterized by sharp signals indicating their diamagnetic nature, as expected for cobalt(III) ions with a low-spin d^6 electronic configuration. The diamagnetic nature of the complexes was also ascertained by our solid-state magnetic susceptibility measurements at room temperature. The spectral data are given in Table 6. The ^{1}H NMR spectrum of **1a** recorded in D_2O shows[13] the presence of only one type of environment for the four acetato ligands as well as the four pyridine ligands. This indicates that the cobalt centers are equivalent in the solution phase. The ^{13}C NMR spectrum of **1a** recorded in D_2O shows resonances of carbon nuclei in five different chemical environments, as expected. The ^{1}H NMR spectrum of **1a**·$KPF_6\cdot 3H_2O$ in D_2O is shown in Figure 7. The resonances for the pyridine ligands appear at 8.14 (d, 8H), 7.66 (t, 4H), and 7.16 (t, 8H) ppm while the methyl protons of acetato ligands appear as a sharp singlet at 2.01 (s, 12H) ppm. For **1b**, this particular methyl resonance for the acetato ligands is found to be downfield-shifted to 2.13 ppm, which is well separated from the other singlet at 2.30 ppm due to the methyl groups at the 4-position of the 4-Mepy ligands. The four pyridine ring protons appear,

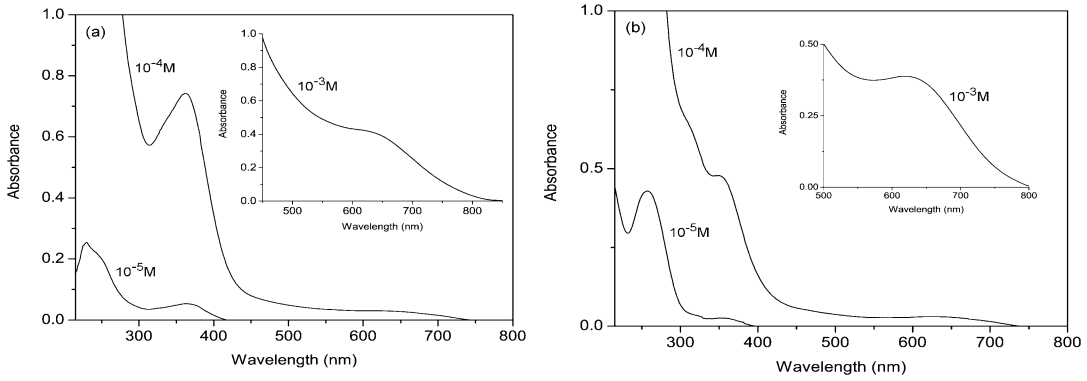

Figure 6. Electronic spectral absorptions for **1a** in (a) CH_2Cl_2 and (b) H_2O based on measurements in 10^{-3}, 10^{-4}, and 10^{-5} M solutions.

Table 6. ^{1}H NMR Chemical Shifts (ppm) for Complexes **1a**−**d**

complex	solvent	δ (L)	δ (CH_3)
1a	D_2O	8.16 (d, J = 4.86 Hz, 8H), 7.69 (t, J = 8.26 Hz, 4H), 7.18 (t, J = 7.02 Hz, 8H)	2.05 (s, 12H)
1a·KPF_6·$3H_2O$	D_2O	8.14 (d, J = 5.08 Hz, 8H), 7.66 (t, J = 7.68 Hz, 4H), 7.16 (t, J = 7.2 Hz, 8H)	2.01 (s, 12H)
1b	$CDCl_3$	8.36 (8H), 6.86 (8H), 2.30 (s, 12H)	2.13 (s, 12H)
1c	$CDCl_3$	8.43 (d, J = 4.7 Hz, 8H), 6.92 (d, J = 4.4 Hz, 8H), 2.58 (q, J = 7.6 Hz, 8H), 1.20 (t, J = 7.5 Hz, 12H)	2.16 (s, 12H)
1d	D_2O	8.41 (d, J = 6.3 Hz, 4H), 7.65 (d, J = 6.0 Hz, 4H)	2.05 (s, 12H)
1d	DMSO-d_6	8.56 (d, J = 6.2 Hz, 8H), 7.69 (d, J = 6.1 Hz, 8H)	1.93 (s, 12H)

however, as two broadened singlets at 8.36 and 6.86 ppm instead of the two expected doublets.

In the ^{1}H NMR spectrum of **1c** recorded in $CDCl_3$, all expected resonances due to the coordinated 4-ethypyridine ligand and the $CH_3CO_2^-$ ligands are observed. The presence of the ethyl group of 4-ethypyridine is indicated by quartet and triplet resonances at 2.58 and 1.20 ppm, respectively. Unlike in the case of compound **1b**, the pyridine ring protons now appear in the form two well-resolved doublets centering at 8.43 and 6.92 ppm, as expected. The methyl group resonance for the bridging acetato ligands is once again downfield-shifted (s, 2.16 ppm).

For **1d**, the spectra have been recorded in D_2O and DMSO-d_6, and in both cases the observed resonances have been assigned. In D_2O, the expected doublets attributable to the 4-cyanopyridine ligands are found at 8.41 and 7.65 ppm. These doublets are observed at 8.56 and 7.69 ppm when DMSO-d_6 is the solvent, and in both cases the coupling constants are close to 6 Hz. The methyl resonances for the spectra recorded in the two solvents, however, differ by 0.12 ppm to suggest significant solvent dependence of the chemical shift for the methyl group of the acetato ligands. Indeed, the same singlet resonances observed for **1b** and **1c** using $CDCl_3$ as the solvent also appear at higher ppm values. These results suggest the appreciable influence of solvents on the geometry of the tetranuclear clusters in solution. This observation is in conformity with UV−vis spectral results on the cluster complexes (vide supra).

Electrochemistry. Electrochemical properties of the tetrameric oxo-bridged complexes **1a**−**d** have been studied by cyclic and differential pulse voltammetric techniques using a three-electrode assembly. The cyclic voltammograms obtained at different scan rates for a MeCN solution of **1a** using a platinum working electrode are shown in Figure 8. A nearly reversible oxidation with $E_{1/2}$ = 0.73 V and ΔE_p = 0.066 V vs Ag/AgCl is observed. The i_{pa}/i_{pc} ratio of ∼1.0 for the oxidation process in **1a** also indicates the reversibility of the couple. The CV scans show well-shaped reverse waves in the 10−100 mV·s^{-1} scan rate range explored. In this range, plots of i_p vs $\nu^{1/2}$ (ν = scan rate) give a straight line (Figure 9), indicating the redox response to be a diffusion-controlled process. The differential pulse voltammetric (DPV) peak potential for complex **1a** is observed at 0.77 V. An $E_{1/2}$ value of 0.78 V is obtained using a glassy-carbon electrode referenced to Ag/AgCl.

Table 7. CV[a] and DPV[b] Data for **1** in CH_2Cl_2/0.1 M TBAP vs SCE

	CV data		
complex	$E_{1/2}$ (V)	ΔE_p (mV)	DPV data (V)
1a	0.73[c]	66	0.77
1a	0.75[d]	170	0.77
1a	0.78[e]	73	
1b	0.71	138	0.73
1c	0.72	140	0.74
1d	1.0	128	1.02

[a] Scan rate, 20 mV·s^{-1}. [b] Scan rate, 5 mV·s^{-1}. [c] In MeCN; working electrode, Pt; reference electrode, Ag/AgCl. [d] In CH_2Cl_2/0.1 M TBAP; working electrode, Pt; reference electrode, Ag/AgCl. [e] In MeCN; working electrode, glassy carbon; reference electrode, Ag/AgCl.

The cyclic voltammogram recorded using a Pt electrode for a MeCN solution of **1a**·$NaClO_4$·$3.5H_2O$ also gave an identical $E_{1/2}$ value of 0.73 V vs Ag/AgCl. This result suggests that the redox active species in this instance is no different from complex **1a**. The complexes **1b**−**d** also display nearly reversible or quasi-reversible redox behavior. The electrochemical data are presented in Table 7. It may be noted that owing to the greater electron-withdrawing ability of the nitrile functionality present in complex **1d**, the observed $E_{1/2}$ value is relatively high for this particular compound.

The stoichiometry of electron transfer determined from the peak current measurements using ferrocene in equimolar concentration as an internal standard shows that the ratio of observed peak currents for ferrocene and **1a** is ∼4 (Figure

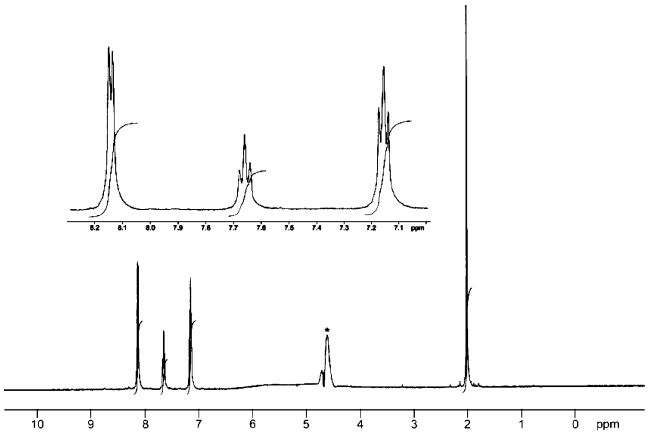

Figure 7. Spectrum of 270 MHz ^{1}H NMR analysis of **1a**·KPF_6·$3H_2O$ in D_2O. The peak marked with an asterisk is due to solvent portion impurity.

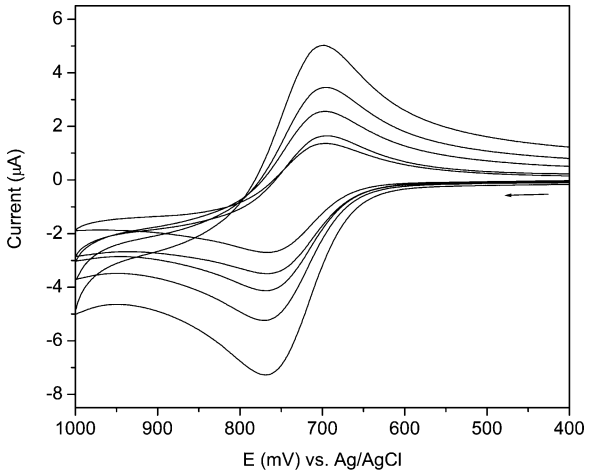

Figure 8. Cyclic voltammograms for **1a** in MeCN/0.2 M TBAP at the scan rates of 10, 20, 30, 50, and 100 mV·s^{-1}.

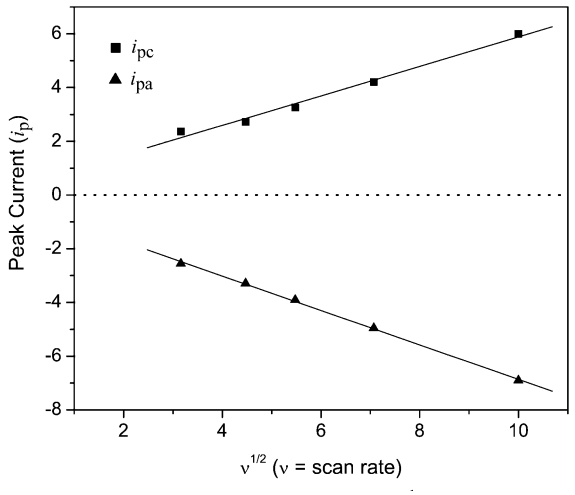

Figure 9. Plot of i_p vs $\nu^{1/2}$ (ν = scan rate) at scan rates of 10−100 mV·s^{-1} for **1a**.

10). This suggests that only one Co^{III} center per "$(Co^{III})_4O_4$" cluster undergoes oxidation. Thus the electron-transfer process involves a one-electron oxidation of the cubane core from $[(Co^{III})_4(\mu_3\text{-}O)_4]^{4+}$ to $[(Co^{III})_3Co^{IV}(\mu_3\text{-}O)_4]^{5+}$ (eq 1). A recent electrochemical study[25] on a structurally related complex $[Co_4(\mu_3\text{-}O)_4(\mu\text{-}O_2CMe)_2(bpy)_2]^{2+}$ in MeCN by Christou et al. revealed a similar oxidation process where

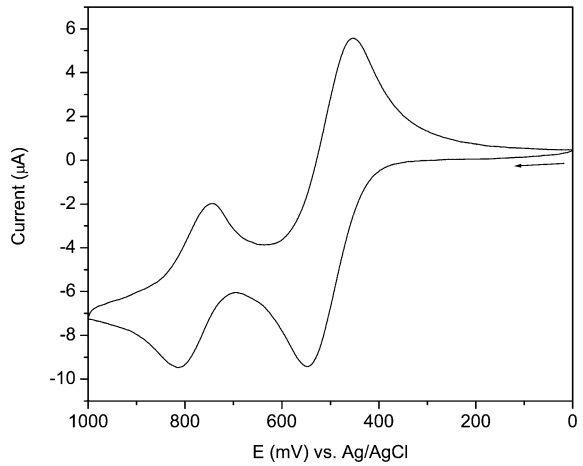

Figure 10. Cyclic voltammogram at 20 mV·s^{-1} on platinum electrode of **1a** in MeCN containing 0.2 M TBAP and ferrocene as an internal standard.

the cubane core $[Co_4(\mu_3\text{-}O)_4]^{4+}$ containing $4Co^{III}$ was oxidized to a $3Co^{III}$, Co^{IV} form.

$$[Co_4{}^{III}O_4(\mu_3\text{-}O)_4(\mu\text{-}O_2CMe)_4(py)_4] \underset{+e}{\overset{-e}{\rightleftharpoons}} [Co_3{}^{III}Co^{IV}O_4(\mu_3\text{-}O)_4(\mu\text{-}O_2CMe)_4(py)_4]^+ \quad (1)$$

Reversible or nearly reversible redox behavior shown by the tetrameric cluster complexes containing a cubane-like $[(Co^{III})_4(\mu_3\text{-}O)_4]^{4+}$ core thus suggests that both the native and oxidized states of the complexes are stable in solution. This indicates that, due to their rather facile oxidizability, complexes of type $Co_4(\mu_3\text{-}O)_4(\mu\text{-}O_2CMe)_4(L)_4$ (**1**) may be suitable as catalysts for the reduction of organic compounds, particularly in view of the fact that many cobalt species are proven oxidation catalysts for various organic substrates.[26]

Scheme 2

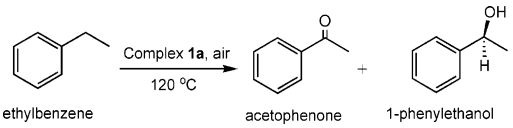

Catalytic Properties. Several reports dealing with the role of metal−oxo clusters in the catalytic oxidation of various industrially important alkylaromatics have been published.[9] We have recently shown that cubane-like cobalt(III) complexes of type $Co_4(\mu_3\text{-}O)_4(\mu\text{-}O_2CR)_4(L)_4$ are catalytically relevant in the oxidation of organic compounds.[11−14] In particular, the complexes **2** and **1d** immobilized on mesoporous silica have been found to show excellent activity in the selective epoxidation of a bicyclic monoterpene, α-pinene.[11,14] Again, **1a** supported on mesoporous silica is an effective heterogeneous catalyst for alcohol oxidation for the selective production of carbonyl compounds.[13] Furthermore, compound **1d** also provides a catalytic system for the homogeneous oxidation of *p*-xylene to form *p*-toluic (4-methylbenzoic) acid under moderate O_2 pressure in an aqueous medium.[12] In this reaction, terephthalic (1,4-ben-

(25) Dimitrou, K.; Brown, A. D.; Concolino, T. E.; Rheingold, A. L.; Christou, G. *Chem. Commun.* **2001**, 1284−1285.
(26) Sheldon, R. A.; Kochi, J. A. *Metal Catalysed Oxidations of Organic Compounds*; Academic Press: New York, 1981.

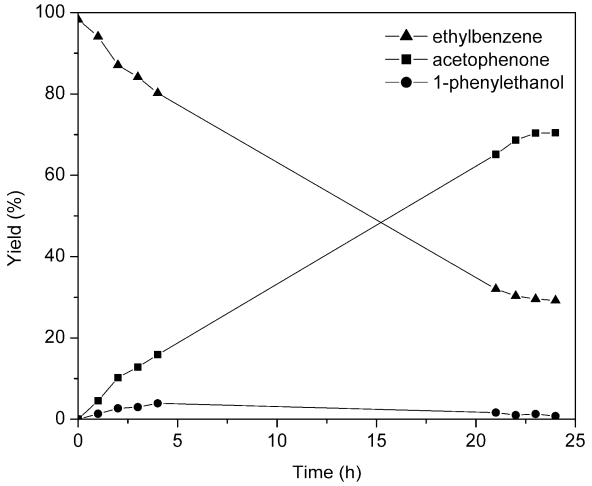

Figure 11. Oxidation of neat ethylbenzene with air under atmospheric pressure in the presence of complex **1a**.

zenedicarboxylic) acid was found to form only in traces. Presently, we report the homogeneous phase aerobic oxidation of ethylbenzene and *p*-xylene in the liquid phase without using any solvents. The presence of **1a** in the reaction mixture is essential for a measurable reaction rate as well as product yield.

With **1a** dissolved in it, neat ethylbenzene undergoes conversion to form acetophenone in ∼69% yield along with a minor amount of 1-phenylethanol (1%) as the other product at the end of 22 h (Scheme 2). A very high selectivity of 99% toward acetophenone is observed. The course of the catalytic reaction is graphically shown in Figure 11.

The conversion of ethylbenzene proceeds more or less linearly with time at the rate of ca. 5% per hour at 120 °C for the first 4 h, and thereafter the rate of oxidation slows down a little, but the rise in conversion remains almost linear up to 22 h, after which the amount of acetophenone levels off. Interestingly, no induction period (time lag before product formation) is observed, in contrast to other cobalt-catalyzed processes. The oxidizing ability of the cobalt(III) cubane complexe **1a** thus appears superior compared with that of other reported systems that use Co-based catalysts for the oxidation of ethylbenzene to acetophenone.[27−29] Łukasiewicz et al. obtained only 6% acetophenone in the presence of chlorobenzene as solvent after 18.5 h under atmospheric pressure using a mixed-valence Co^{II}/Co^{III} trimer.[30] Similar homogeneous liquid-phase oxidation using a Co(II)−Schiff-base complex also led to a low yield of acetophenone.[31] Product selectivities are also much better with our cubane complexes even compared to the Co(III)

Scheme 3

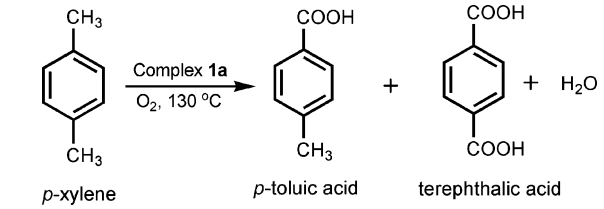

complexes, which are reported[27] to be highly active in the oxidation of ethylbenzene to acetophenone at 150 °C. The acetophenone productivity calculated for the present study is 2310 mol per mole of complex **1a**, while the turnover frequency calculated for the first 4 h of the reaction is 212 h^{-1}. These figures are also significantly higher compared with the results obtained using Co(III)-based catalysts.[27] The present result obtained by us under homogeneous conditions by making use of a cobalt(III) cubane cluster also compares well with the highly active heterogeneous catalyst, also based on a Co(III)−oxo species.[15]

Metal-catalyzed oxidation of ethylbenzene usually proceeds through a radical chain process. The mechanism by which cobalt(III) complexes initiate the chain process is likely to involve alkylperoxy radicals as intermediates.[28] The initiation is considered to involve hydrogen abstraction from the hydrocarbon by Co(III) species. In view of the facile one-electron oxidation shown by complex **1a** and its analogues, a complex species containing Co(IV) is expected to be involved in the present catalytic process. Mechanistic aspects of the reported reactions, however, need to be studied further.

Complex **1a** has also been found to be useful in the autoxidation of *p*-xylene with air under atmospheric pressure and in the absence of any cocatalysts or additives under solvent-free conditions (Scheme 3). As described in the Experimental Section, the autoxidation of *p*-xylene has been carried out by passing compressed air through the reaction vessel under vigorous stirring. The formation of solid product starts immediately. As the product builds up in the flask, mechanical stirring as well as airflow becomes hindered. After 7 h, the isolated yields of *p*-toluic acid and terephthalic acid are found to be ∼24 and ∼1%. Compound **1d** under moderate O_2 pressure in an aqueous medium under homogeneous condition had earlier led to the formation of *p*-toluic acid as the main product with only traces of terephthalic acid as the other product.[12] Our results thus indicate that the cobalt(III)−oxo clusters may be active as catalysts for *p*-xylene oxidation in highly polar (water) as well as nonpolar (*p*-xylene) media.

Typically, cobalt-catalyzed autoxidation of *p*-xylene in the liquid phase is carried out in an acetic acid medium at very high temperature (195−205 °C) and pressure (∼30 bar) in the presence of a halide ion promoter that significantly changes the reaction kinetics of such processes.[29] Since the oxidation of Co(II) to Co(III) is a slow process, the use of promoters is necessary in cobalt(II)-catalyzed processes to prevent a possible induction period during which no desired conversion takes place. The absence of induction period and promoters and the dispensability of solvents in the presently

(27) Qi, J.-Y.; Ma, H.-X.; Li, X.-J.; Zhou, Z.-Y.; Choi, M. C. K.; Chan, A. S. C.; Yang, O.-Y. *Chem. Commun.* **2003**, 1294−1295.
(28) Budnik, R. A.; Kochi, J. A. *J. Org. Chem.* **1976**, *41*, 1384−1389.
(29) (a) Partenheimer, W. *Catal. Today* **1995**, *23*, 69−158. (b) Suresh, A. K.; Sharma, M. M.; Sridhar, T. *Ind. Eng. Chem. Res.* **2000**, *39*, 3958−3997. (c) Raghavendrachar, P.; Ramachandran, S. *Ind. Eng. Chem. Res.* **1992**, *31*, 453−462.
(30) Łukasiewicz, M.; Ciunik, Z.; Mazurek, J.; Sobczak, J.; Staroń, A.; Wołowiec, S.; Ziółkowski, J. J. *Eur. J. Inorg. Chem.* **2001**, 1575−1579.
(31) Punniyamurthy, T.; Bhatia, B.; Reddy, M. M.; Maikap, G. C.; Iqbal, J. *Tetrahedron* **1997**, *53*, 7649−7670.

reported reactions are significant because these factors may be helpful in the achievement of green chemistry goals.

Conclusion

Tetrameric cubane-like complexes $Co_4(\mu_3\text{-}O)_4(\mu\text{-}O_2CMe)_4L_4$ with L = pyridine, 4-methylpyridine, 4-ethylpyridine, and 4-cyanopyridine have been prepared by a single-step procedure involving the H_2O_2 oxidation of Co^{2+} in presence of appropriate ligands. Cocrystallizing alkali-metal salts influence the crystal structure of $Co_4(\mu_3\text{-}O)_4(\mu\text{-}O_2CMe)_4(py)_4$ due to supramolecular effects. The olive-green complexes of cobalt(III) dissolve in many common solvents to give rise to stable solutions. The clusters undergo reversible one-electron oxidation involving the $[(Co^{III})_4(\mu_3\text{-}O)_4]^{4+}/[(Co^{III})_3Co^{IV}(\mu_3\text{-}O)_4]^{5+}$ redox couple with $E_{1/2} \leq 1$ V. Solutions of the complex $Co_4(\mu_3\text{-}O)_4(\mu\text{-}O_2CMe)_4(py)_4$ in the substrate catalyze the side-chain oxidation of neat ethylbenzene and *p*-xylene with air as the oxidant. Excellent selectivity for acetophenone is observed in the oxidation of ethylbenzene.

Acknowledgment. Financial assistance from DST, Government of India (Grant No. SR/S1/IC-51/2003) is gratefully acknowledged. Thanks are due to single-crystal X-ray diffraction facilities at Indian Institute of Science (Bangalore) and Indian Institute of Technology (Guwahati) for providing us with the intensity data. R.C. thanks University Grants Commission, India, for a Research Fellowship. The authors also thank Prof. J. H. Clark of the University of York, U.K. for his help and suggestions in doing the catalytic work.

Supporting Information Available: Listings of complete structural results on **1a**·$0.5NaNO_3$·$8H_2O$ (CCDC 632027), **1a**·$NaClO_4$·$3.5H_2O$ (CCDC 650129), and **1b**·$3H_2O$ (CCDC 650128) in CIF format; ^1H and ^{13}C NMR spectra of **1a**, TG curve of **1a**·$0.5NaNO_3$·$8H_2O$, and ESI-MS graph of **1d** in TIF format. This material is available free of charge via the Internet at http://pubs.acs.org.

IC7011759